Colloid & Polymer Science Colloid Polym Sci 272:1582–1589 (1994)

Sedimentation equilibrium of suspensions of colloidal particles at finite concentrations

M. Martin[1]), M. Hoyos[1]), and D. Lhuillier[2])

[1]) Ecole Supérieure de Physique et Chimie Industrielles, Laboratoire de Physique et Mécanique des Milieux Hétérogènes (URA CNRS 857) Paris, France
[2]) Université Pierre et Marie Curie, Laboratoire de Modélisation en Mécanique (URA CNRS 229). Paris, France

Abstract: Equilibrium concentration profiles of non-dilute colloidal suspensions are calculated by means of the Carnahan–Starling expression for the osmotic compressibility of hard sphere liquids. The profiles depend on the average volume fraction of the suspension, $\langle\phi\rangle$, and on the field interaction parameter, λ_0 (reciprocal of the Péclet number at infinite dilution). Profiles are computed for values of $\langle\phi\rangle$ and λ_0 typical of those encountered in sedimentation field-flow fractionation experiments. It is found that, in most cases, the volume fraction at the depletion wall is negligibly small and that the volume fraction at the accumulation wall, ϕ_0, depends on the ratio $\langle\phi\rangle/\lambda_0$ only. An inflexion point is found in the concentration profile if ϕ_0 is larger than 0.13, whatever the value of λ_0.

Key words: Sedimentation equilibrium – colloidal particles – hard spheres – finite concentrations

Introduction

The sedimentation of particulate materials is a ubiquitous and important phenomenon of environmental, biological, and industrial relevance. In a batch sedimentation process of an initially uniform suspension, one usually encounters three zones, both in transient and equilibrium conditions [1]. At the bottom of the vessel, a sedimentation cake is formed with a volume fraction which somewhat depends on the compressibility of the packing and is about 0.6. Above that sediment layer, one finds a transition layer, the height of which varies during the settling process and depends on the diffusivity of the particles. Then, a clear liquid is found above that layer. The relative importance of the three zones depends on the average volume fraction of the suspension, but also on the height of the sedimentation vessel. Many studies have focussed on the dynamics of the sedimentation process in situations where the height of the sedimentation vessel is large enough for a sediment to be formed. The theory of the transient batch settling for noncolloidal particles was first formulated by Kynch [2]. This theory has been recently extended by Davis and Russell [3] to account for the influence of the Brownian motion of the particles on the transition layer above the sediment.

There are situations, however, where the vessel height is so small that a compact sediment is never obtained in spite of the relatively large average volume fraction of the suspension. Such is the case, for instance, in field-flow fractionation (FFF) experiments. FFF is an analytical method for separation and characterization of supramolecular materials. The separation occurs during the transportation, by means of a carrier liquid, of the particulate sample through a thin, ribbon-like channel under the influence of an external field applied perpendicularly to the main plates of the channel [4]. In usual operating conditions, the carrier flow velocity is small and the mean residence time of the particles depends on the

equilibrium concentration distribution in the field direction. It is therefore of major interest to know this distribution for separation optimization as well as for particle characterization.

When the suspension is highly dilute and the field is constant throughout the channel thickness, the concentration decreases exponentially from the accumulation plate [5]. For less dilute suspensions, the volume fraction near the accumulation plate can be large enough for deviations from the exponential profile to occur.

The objective of the present study is to determine the equilibrium concentration profile for a suspension submitted to a constant field when the volume fraction near the accumulation wall is large enough for interactions between particles to be significant. This is the case of most FFF experiments with not too dilute samples.

Theory

One considers a suspension of identical Brownian particles in a quiescent fluid enclosed in a vessel between two parallel plates (the plates are assumed to be large enough for side wall effects to be negligible). A gravitational field is applied in the direction perpendicular to the plates. The acceleration of this gravitational field, G, is assumed to be constant throughout the vessel. This assumption is obviously correct for experiments performed with the Earth's gravitational field. It is mostly correct for centrifugal FFF experiments since the distance between the two rotating plates is much smaller than their mean distance to the rotation axis (in typical instruments, the variation of G through the channel thickness is less than 0.2%). For the same reason, the centrifugal sedimentation can be assumed to be a one-dimensional problem as in the Earth gravitational experiment.

General expression of the volume fraction profile

The effective force, F_{ext}, exerted by the gravitational field on a particle of volume v_p is the body force corrected by the Archimedes force:

$$F_{ext} = v_p \rho_p G - v_p \nabla_p \,, \qquad [1]$$

where ρ_p is the mass per unit volume of particles and ∇_p the hydrostatic pressure gradient in the suspension, given by:

$$\nabla_p = [\phi \rho_p + (1 - \phi)\, \rho_f] G \,, \qquad [2]$$

ρ_f is the mass per unit volume of the suspending fluid, and ϕ is the volume fraction of the particles. Here, bold-face symbols represent vectorial quantities. Combining Eqs. (1) and (2) and defining $\Delta_p = \rho_p - \rho_f$, one finds:

$$F_{ext} = (1 - \phi)\, v_p \Delta\rho G \,. \qquad [3]$$

Each particle is also submitted to a thermodynamic force, F_{th}, linked to the gradient of the chemical potential per particle, $\mu_p(p, T, \phi)$. This chemical potential is the sum of two contributions: the bare particle contribution, $\mu_p^0(p, T)$, at the same pressure and temperature as the suspension, and the excess (or mixing) chemical potential $\Delta\mu_p(p, T, \phi)$. For rigid particles with hard-core interactions, $\Delta\mu_p$ depends only on the particle volume fraction. When ϕ is not uniform over the suspension, the force acting on a particle is:

$$F_{th} = -\frac{\partial \Delta\mu_p}{\partial\phi} \nabla\phi \,. \qquad [4]$$

The chemical potential of a fluid molecule, μ_f, can also be written as the sum $\mu_f = \mu_f^0 + \Delta\mu_f$. As a consequence of the Gibbs–Duhem relationship between $d\mu_p$, $d\mu_f$, dp and dT, the variations with ϕ of $\Delta\mu_f$ and $\Delta\mu_p$ are related by [6a] :

$$c_p \frac{\partial \Delta\mu_p}{\partial\phi} + c_f \frac{\partial \Delta\mu_f}{\partial\phi} = 0 \,, \qquad [5]$$

where c_p and c_f are the numbers of particles and of fluid molecules per unit volume of suspension, respectively. It is usual to express F_{th} as a function of the osmotic pressure, Π, a quantity simply related to the fluid excess chemical potential as [6b] :

$$\frac{\partial \Delta\mu_f}{\partial\phi} = -v_f \frac{\partial \Pi}{\partial\phi} \,, \qquad [6]$$

where v_f is the volume of a fluid molecule. Noting that $c_f v_f = 1 - \phi$ and $c_p v_p = \phi$, one can combine Eqs. (4) to (6) to obtain:

$$F_{th} = -\frac{1 - \phi}{\phi} v_p \frac{\partial \Pi}{\partial\phi} \nabla\phi \,. \qquad [7]$$

In equilibrium condition, the effective external force and the thermodynamic force exactly balance each other:

$$F_{ext} + F_{th} = 0 \,, \qquad [8]$$

which gives the basic expression for the volume fraction profile at equilibrium :

$$\frac{\nabla\phi}{\phi} = \Delta\rho \frac{G}{\partial\Pi/\partial\phi} \,. \qquad [9]$$

Introducing the osmotic compressibility factor, Z, defined as:

$$Z = \frac{\Pi}{c_p kT} \,, \qquad [10]$$

where k is the Boltzmann constant and T the absolute temperature, and noting that $\phi Z = \Pi v_p/kT$, Eq. (9) can be written as :

$$\frac{\partial(\phi Z)}{\partial\phi}\frac{\nabla\phi}{\phi} = \frac{v_p \Delta\rho G}{kT} \,. \qquad [11]$$

The absolute value of the right-hand side of Eq. 11 can be written as $1/(\lambda_0 w)$, where w is the cell height (distance between the two plates) and λ_0 a dimensionless field interaction parameter (the basic FFF parameter) which is nothing else than the reciprocal of a Péclet number, Pe:

$$\lambda_0 = \frac{kT}{v_p|\Delta\rho G|w} = \frac{kT}{|F_0|w} = \frac{D_0}{|U_0|w} = \frac{1}{\mathrm{Pe}} \,. \qquad [12]$$

Here, D_0 is the diffusion coefficient of the particles, U_0 their sedimentation velocity, and F_0 the effective force exerted by the field on a single particle, while the subscript "0" refers to the infinite dilution limit. If the x-axis is oriented from the accumulation plate towards the depletion plate, $\Delta\rho\, G$ is negative and Eq. (11) can be rewritten as:

$$\partial\frac{(\phi Z)}{\partial\phi}\frac{d\phi}{\phi} = -\, d\left(\frac{x/w}{\lambda_0}\right) \qquad [13]$$

This is the basic differential equation governing the volume fraction profile.

The solution of that equation is :

$$F(\phi) = F(\phi_0) - \frac{x/w}{\lambda_0} \,, \qquad [14]$$

where $\phi dF/d\phi = \partial(\phi Z)/\partial\phi$, while ϕ_0 is the particle volume fraction at the accumulation plate ($x = 0$). As a consequence, the value ϕ_1 of the particle volume fraction at the depletion plate ($x = w$) is a function of λ_0 and ϕ_0 defined by:

$$F(\phi_1) \;= F(\phi_0) - \frac{1}{\lambda_0} \,. \qquad [15]$$

There is a second relationship between ϕ_1 and ϕ_0 expressing the mass conservation of the particles in the sedimentation cell. Let us introduce the average volume fraction:

$$\langle\phi\rangle = \int_0^1 \phi\, d(x/w) \;. \qquad [16]$$

Taking Eq. (13) into account, one obtains:

$$\phi_0 Z(\phi_0) - \phi_1 Z(\phi_1) = \frac{v_p}{kT}(\Pi(\phi_0) - \Pi(\phi_1)) = \frac{\langle\phi\rangle}{\lambda_0} \,. \qquad [17]$$

Solving Eqs. (15) and (17) gives the values of ϕ_0 and ϕ_1 as a function of λ_0 and $\langle\phi\rangle$. Hence, the equilibrium profile given by Eq. (14) is ultimately a function of $x/w\lambda_0$, λ_0 and $\langle\phi\rangle$.

A well-known peculiar solution corresponds to a very dilute suspension for which $Z \approx 1$ for any volume fraction in the range $\phi_1 < \phi < \phi_0$. In this case, one has:

$$\phi = \phi_0 \exp\left(-\frac{x/w}{\lambda_0}\right), \qquad [18]$$

and:

$$\phi_0 = \frac{\langle\phi\rangle}{\lambda_0(1 - \exp(-1/\lambda_0))} \qquad [19]$$

For large Péclet numbers ($\lambda_0 \ll 1$), the concentration decreases rapidly with increasing distances from the accumulation plate, and one finds for ϕ_1 a value much smaller than ϕ_0 which, in this case, is equal to $\langle\phi\rangle/\lambda_0$. There is a reminiscence of this peculiar behavior for a non-dilute suspension: if $\lambda_0 \ll 1$, it is clear from Eq. (17) that $\phi_0 Z(\phi_0)$ should be much larger than $\phi_1 Z(\phi_1)$, and, in most cases, this implies $\phi_1 \ll \phi_0$ (cf. Fig. 1 below). Then, the volume fraction at the accumulation plate is a function of $\langle\phi\rangle/\lambda_0$ only, and the concentration profile depends on $\langle\phi\rangle/\lambda_0$ and no longer on $\langle\phi\rangle$ and λ_0 separately. Note also that, in the limit of a vanishingly small value of λ_0, the only possible profile is one with $\phi_1 = 0$ and $\phi_0 = \phi_{max}$,

where ϕ_{max} is the volume fraction for which Z becomes infinite, i.e., the volume fraction of the incompressible sedimentation cake. We are here mostly interested in cases where ϕ_0 is likely to be smaller than ϕ_{max}, hence when $\langle\phi\rangle/\lambda_0$ is itself smaller than ϕ_{max}. According to Eq. 12, this happens when the product $\langle\phi\rangle|F_0|w$ is small, i.e., for small cell heights and/or small field strengths and/or not too concentrated suspensions.

Osmotic compressibility of a hard sphere suspension

Most of what is known about $Z(\phi)$ comes from early studies of hard sphere liquids. There exist theoretical predictions concerning the two limit cases $\phi \ll 1$ (hard-sphere gas, virial expansion [7]) and $\phi \approx \phi_{max}$ (dense hard-sphere liquid, free-volume expansion [8]), as well as numerical results covering the whole range $0 < \phi < \phi_{max}$. Some phenomenological expressions of $Z(\phi)$ have been proposed to reproduce these results as closely of possible. The most favored is the semi-empirical one devised by Carnahan and Starling [9] :

$$Z(\phi) = 1 + \frac{2\phi(2-\phi)}{(1-\phi)^3}. \qquad [20]$$

This expression gives amazingly good predictions for volume fractions up to 40% [10] and describes satisfactorily the physical properties of monodisperse sols of spherical particles [11]. It agrees with both the first seven virial coefficients, computed from statistical mechanics arguments, and the molecular dynamics results [1, 12]. One of its obvious drawbacks is its divergence for $\phi = 1$ while this behavior is expected for $\phi = \phi_{max} \approx 0.6$. Hence, we will accept the predictions of Eq. (20) provided the predicted value of ϕ_0 is smaller than 0.4 approximately. The above expression for Z leads to a concentration profile given implicitly by Eq. (14) with:

$$F(\phi) = \ln\phi + \frac{3-\phi}{(1-\phi)^3}. \qquad [21]$$

The term beside $\ln\phi$ in this equation is always positive. Accordingly, as a consequence of the excluded volume (hard-core) interactions between particles, the concentration profile decreases less rapidly than the exponential profile. The variations of $F(\phi)$ and of $\phi Z(\phi)$ for the Carnahan–Starling compressibility expression are shown in Fig. 1 together with the corresponding curves for $Z = 1$, which would lead to the exponential concentration profile.

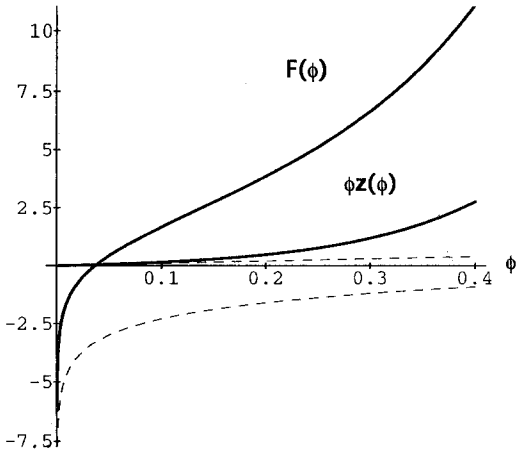

Fig. 1. Variations of $\phi Z(\phi)$ (solid curve a) and of $F(\phi)$ (solid curve b) versus the volume fraction of the suspension, ϕ, for the Carnahan–Starling expression of the compressibility factor. The dashed curves correspond to $Z = 1$

Results and discussion

The above approach for obtaining the volume fraction profile of a steady-state suspension in a gravitational field is similar to the approaches followed by Vrij [13] and by Davis and Russel [3]. Because they were mostly interested in the description of the behavior of the suspension in and near the sediment cake, Davis and Russel used an asymptotic form of the osmotic compressibility factor at large volume fractions. It cannot accurately describe the concentration profile in the entire volume fraction range. Vrij, treating the steady-state sedimentation profile in a centrifugal field with a varying G, used the Carnahan–Starling equation and obtained an expression similar to Eqs. (21) and (14). In the above treatment, the integration constant problem raised by Vrij was solved by numerical determination of ϕ_0 and ϕ_1 in terms of $\langle\phi\rangle$ and λ_0, by solving Eqs. (15) and (17). This allows to plot volume fraction profiles for different sets of experimental conditions.

The determination of the concentration profile requires first the determination of ϕ_0 and ϕ_1 in

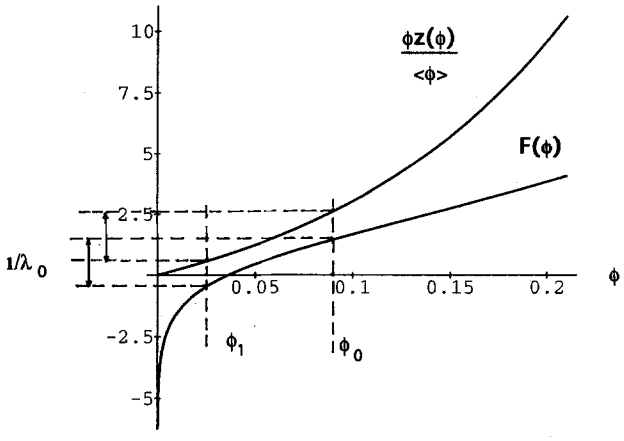

Fig. 2. Variations of $\phi Z(\phi)/\langle\phi\rangle$ (upper curve) and $F(\phi)$ (lower curve) versus ϕ, for $\langle\phi\rangle = 0.05$. Graphical procedure for the determination of the volume fractions at the accumulation and depletion plates, ϕ_0 and ϕ_1, respectively, when $1/\lambda_0$ is equal to 2. ϕ_0 and ϕ_1 are determined in such a way that the differences in the ordinates corresponding to these two values are equal to $1/\lambda_0$ for the two curves

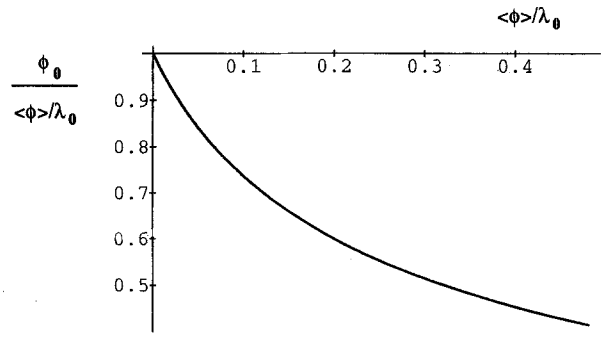

Fig. 3. Ratio of the volume fraction at the accumulation wall, ϕ_0 to $\langle\phi\rangle/\lambda_0$ versus $\langle\phi\rangle/\lambda_0$ when the volume fraction at the depletion wall is negligibly small

terms of $\langle\phi\rangle$ and λ_0. For this purpose, Vrij suggested a graphical method based on surface area determination [13]. Taking into account the properties of Eqs. (15) and (17), an alternative graphical method consists in finding two values of the particle volume fraction such that the same difference $1/\lambda_0$ is obtained for $F(\phi_0) - F(\phi_1)$ and $[\phi_0 Z(\phi_0) - \phi_1 Z(\phi_1)]/\langle\phi\rangle$. This procedure, based on length determination, is more convenient to use than that proposed by Vrij. This procedure is demonstrated in Fig. 2, which shows the variations of $F(\phi)$ and of $\phi Z(\phi)/\langle\phi\rangle$ with ϕ, for $\langle\phi\rangle = 0.05$ and $\lambda_0 = 0.5$, which gives $\phi_0 = 0.090$ and $\phi_1 = 0.024$. This λ_0 value is quite larger than typical values encountered in FFF experiments. When λ_0 is smaller than 0.2, ϕ_1 becomes negligible and, as discussed above, ϕ_0 is such that $\phi_0 Z(\phi)$ is equal to $1/\lambda_0$ and can be directly determined from the $\phi Z(\phi)$ vs. ϕ curve. In the following, in order to plot the volume fraction profiles for different sets of experimental conditions, ϕ_0 and ϕ_1 are computed by numerically solving both Eqs. (15) and (17).

Generally, in sedimentation experiments, as well as for all cases of interest in FFF, when the field strength is large enough for retention to be significant, ϕ_0 is much larger than ϕ_1, so that Eq. (17) can be simplified by neglecting all terms in ϕ_1. The resulting error is smaller than 0.04% in the most extreme case treated below ($\langle\phi\rangle = 10\%$, $\lambda_0 = 0.1$). It thus appears that the maximum volume fraction in the channel, ϕ_0, depends only on the ratio $\langle\phi\rangle/\lambda_0$, but not on the specific values of $\langle\phi\rangle$ and λ_0. As discussed above, the limiting value of ϕ_0 at high dilution is, in these conditions, equal to $\langle\phi\rangle/\lambda_0$. The deviation of $\phi_0/(\langle\phi\rangle/\lambda_0)$ from 1 with increasing values of $\langle\phi\rangle/\lambda_0$ is plotted in Fig. 3, when ϕ_1 can be neglected (i.e., when λ_0 is low). As expected, ϕ_0 is seen to increase more slowly than $\langle\phi\rangle$ when λ_0 is kept constant.

The volume fraction profiles are plotted in Fig. 4 as the relative distance from the accumulation wall versus the volume fraction for average volume fractions increasing from 1% (lower curves) to 10% (upper curves). Since, even for the largest $\langle\phi\rangle$, the volume fraction at the depletion wall is nearly zero, the areas below the curves represent the average volume fractions. Accordingly, curves appear to lie above each other when $\langle\phi\rangle$ increases. Interestingly, the figure shows the progressive deviation of the distribution from the exponential profile as the average volume fraction increases. This deviation appears to be more pronounced when λ_0 is smaller (Fig. 4B for $\lambda_0 = 0.01$ compared to Fig. 4A for $\lambda_0 = 0.1$). This is expected since lower λ_0 values lead to higher concentrations at the accumulation wall and thus to stronger excluded volume interactions. However, the accuracy of the profiles must be regarded with some caution when ϕ exceeds about 40% as the Carnahan–Starling expression of the osmotic compressibility factor may not be correct at larger volume fractions. As one approaches the

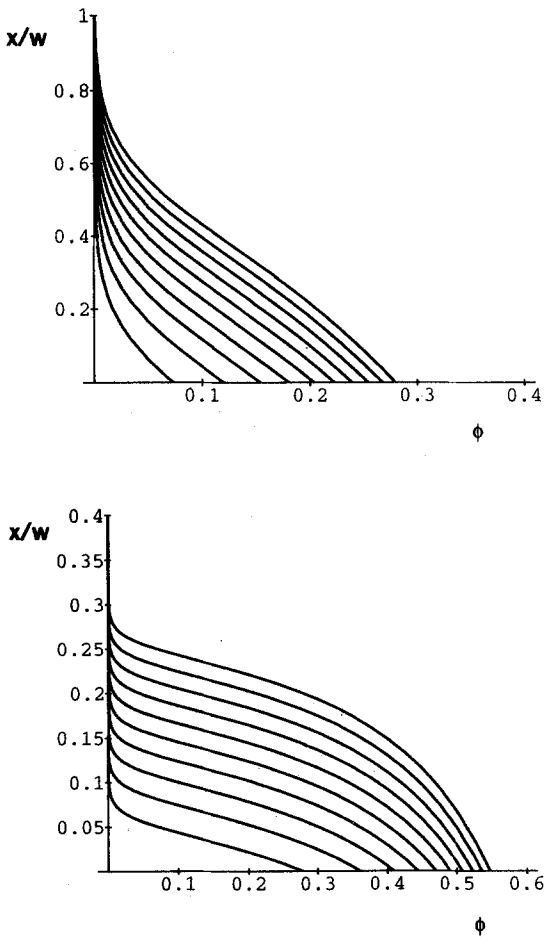

Fig. 4. Volume fraction profiles, plotted as x/w versus ϕ, for various average volume fractions: $\langle\phi\rangle$ = 1%, 2%, 3%, 4%, 5%, 6%, 7%, 8%, 9%, 10% from lower curve to upper curve. (a) $\lambda_0 = 0.1$. (b) $\lambda_0 = 0.01$

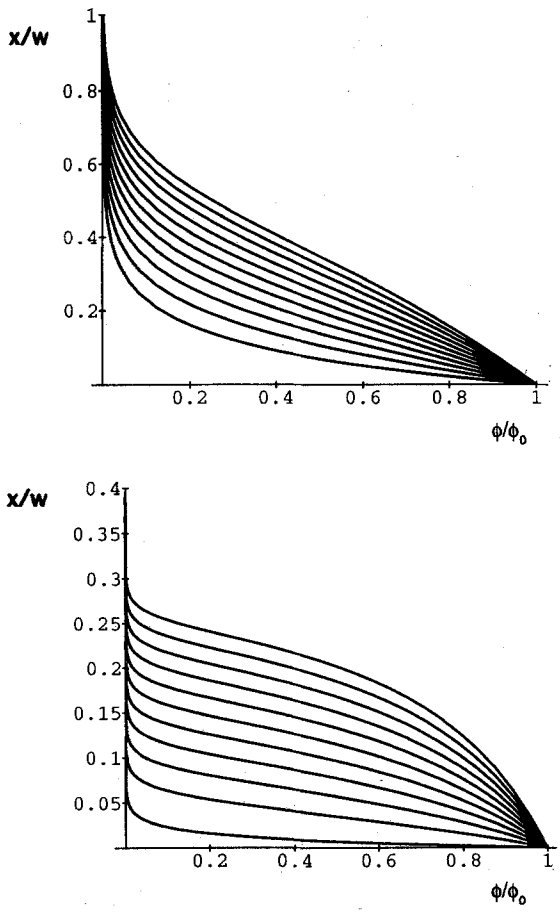

Fig. 5. Relative volume profiles, plotted as x/w versus ϕ/ϕ_0, for various average volume fractions: $\langle\phi\rangle$ = 0%, 1%, 2%, 3%, 4%, 5%, 6%, 7%, 8%, 9%, 10% form lower curve to upper curve. (a) $\lambda_0 = 0.1$. (b) $\lambda_0 = 0.01$

concentration of the sedimentation cake, an asymptotic form of $Z(\phi)$ diverging at the volume fraction of the sediment such as the one used by Davis and Russell [3] would be more appropriate.

It is interesting to observe the variations of the relative volume fraction profiles, ϕ/ϕ_0, as a function of the average volume fraction as they more directly reflect the influence of the hard sphere interactions between particles. Indeed, if there were no such interactions, i.e., if the osmotic compressibility was constant, then the profile would be exponential. Figure 5 shows the deviation of the relative volume fraction profile from the exponential shape for the same values of $\langle\phi\rangle$ and λ_0 as in Fig. 4. The exponential curve obtained for a vanishingly small average volume fraction is also plotted in Figs. 5A and B. The profiles are seen to be considerably distorted when $\langle\phi\rangle$ is large and λ_0 small.

For highly concentrated suspensions, it is clear that there is an upper limit for the volume fraction, since ϕ cannot exceed the volume fraction of a dense packing (from about 58% for the random packing found in sedimentation cake to 74% for the compact hexagonal lattice). If the average particle concentration in the vessel is quite large and F_0 is also large (low λ_0), one can even have the formation of a cake with a nearly constant volume fraction close to the packing value. This is the situation investigated by Russel and Davis [3]. In that case, the curvature of the relative volume fraction profile is negative near the

accumulation wall. However, sufficiently far away from this wall, the suspension becomes diluted enough and the volume fraction decreases again nearly exponentially with increasing distances from the accumulation wall. Then the curvature of the volume fraction profile is positive. Therefore, a position will be found in the intermediate region, where the curvature is zero. At this inflexion point, one has $d^2(x/w)/d\phi^2 = 0$. The volume fraction, ϕ_{infl}, corresponding to the inflexion point is, from Eqs. (14) and (21), found to be the solution of :

$$1 - 5\phi_{infl} - 20\phi_{infl}^2 - 4\phi_{infl}^3 + 5\phi_{infl}^4 - \phi_{infl}^5 = 0 . \quad [22]$$

It is interesting to note that this critical volume fraction is independent of λ_0 and hence on the intensity of the field force. The numerical solution of this equation gives :

$$\phi_{infl} = 0.13044 . \quad [23]$$

This value is very close so that observed by Vrij [13]. Accordingly, an inflexion in the volume fraction profile of the suspension will be found in the vessel if both $\phi_0 > \phi_{infl}$ and $\phi_1 < \phi_{infl}$. In practice, since, as noted above, there is a biunivocal relationship between ϕ_0 and $\langle\phi\rangle/\lambda_0$, the second of these conditions will always be fulfilled while the first, in effect, states that an inflexion in the concentration profile will be found if:

$$\langle\phi\rangle > 0.2272\,\lambda_0 . \quad [29]$$

The influence of λ_0 on the volume fraction profile is seen in Fig. 6 for two average volume fractions (1% and 10% for Figs. 6A and B, respectively). Since, for a given figure, the areas below all curves are constant (as $\langle\phi\rangle$ is fixed) and the volume fraction at the accumulation wall increases with increasing λ_0, the curves for different λ_0 cross each other. Accordingly, a low volume fraction is found at a higher distance from the accumulation wall when λ_0 is larger, while the opposite is true for intermediate or high volume fractions. It is clear in this Figure that, for a given $\langle\phi\rangle$, the stronger the field interaction parameter, the more the concentration profile deviates from the exponential shape.

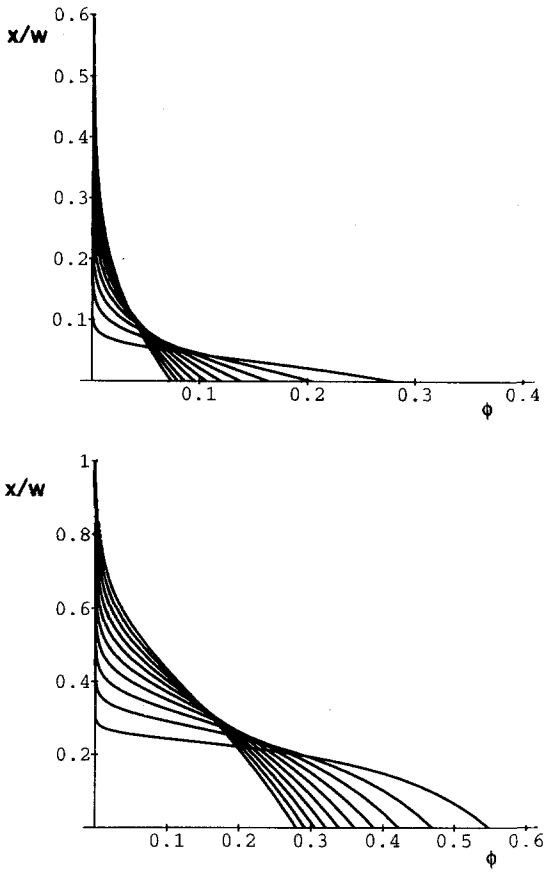

Fig. 6. Volume fraction profiles, plotted as x/w versus ϕ, for various field interaction parameters: $\lambda_0 = 0.01$, 0.02, 0.03, 0.04, 0.05, 0.06, 0.07, 0.08, 0.09, 0.1 from lower to upper curves on the left part of the graph (i.e. from upper to lower curves on the right part of the graph). (a) $\langle\phi\rangle = 1\%$. (b) $\langle\phi\rangle = 10\%$

Conclusion

In the above approach, the Carnahan–Starling expression of the compressibility factor of hard sphere liquids has been used to derive and compute the volume fraction profiles of suspensions in equilibrium conditions. Although the hard sphere hypothesis is unrealistic for most suspensions in which van der Waals and electrostatic interactions cannot be neglected, the Carnahan–Starling expression can still be used. The clue is to replace the volume fraction ϕ by some effective volume fraction, ϕ_{eff}, computed from an effective diameter taking into account the variation of the interaction potential with the interparticle distance [1, 6, 12]. Such a procedure is correct if repulsive forces

are dominant. In cases of attractive forces, the only possibility is to write $Z(\phi, T) = Z_{CS}(\phi) - \chi(T)\,\phi$ where $Z_{CS}(\phi)$ is the Carnahan–Starling compressibility factor given by Eq. (20) and χ is a positive parameter simulating the attraction. Such a procedure was adopted for ferrocolloids [14]. It leads to phase separation when χ exceeds some critical value.

In the above model, the gravitational field has been assumed to be independent of the distance from the accumulation wall. This situation is encountered in natural gravity sedimentation as well as in sedimentation FFF channels for which the channel thickness is much smaller than the mean distance from the rotation axis. However, as shown by Vrij [13], the above results for the volume fraction profiles can be applied to centrifugation experiments provided that the relative distance from the wall, x/w, in Eq. (14) is replaced by $(r_0^2 - r^2)/(r_0^2 - r_i^2)$, where r is the distance to the rotation axis, and r_0 and r_i are the distances of the outer wall and inner wall (or meniscus) to the rotation axis, respectively. In Eq. (12) expressing the field interaction parameter, w then represents $(r_0 - r_i)$ and the acceleration G has to be taken at the channel center as $\omega^2(r_0 + r_i)/2$, where ω is the angular velocity of the channel.

The profiles described in Figs. 3–5 depend on the field interaction parameter and on the average volume fraction. The particle diameter does not influence these profiles on its own, but only through its influence on λ_0 and $\langle\phi\rangle$. This model has obviously some limit, especially near the accumulation wall where particles are sterically excluded. Biben et al. have recently shown that these steric interactions induce oscillatory variations of the density profile near the wall, which are progressively damped with increasing distances from the wall [15]. Furthermore, in this damped domain, they found a fairly good agreement between the profiles obtained from Monte–Carlo simulations and those calculated by means of the Carnahan–Starling compressibility expression.

It is clearly seen in Fig. 5 that, given λ_0, the mean distance of the particles to the accumulation wall is, for any finite $\langle\phi\rangle$, larger than that predicted for the exponential profile and that it increases with increasing $\langle\phi\rangle$. Accordingly, in FFF experiments where the sedimented suspension is transported in quasi-equilibrium conditions, by a laminar flow parallel to the walls, one expects that concentrated suspensions will move faster than diluted suspensions, since the velocity of the flow streamlines increases with increasing distances from the wall. However, this effect can be counteracted by the increased viscosity of concentrated suspensions which reduces the flow velocity near the accumulation wall. The interplay between these two effects on the resulting axial velocity of suspensions will be studied in a forthcoming publication.

References

1. Russel WB, Saville DA, Schowalter WR (1989) Colloidal-Dispersions. Cambridge University Press, Cambridge
2. Kynch GJ (1952) Trans Faraday Soc 48:166–176
3. Davis KE, Russel WB (1989) Phys. Fluids A 1:82–100
4. Giddings JC (1966) Sep Sci 1:123–125
5. Giddings JC (1968) J Chem Phys 49:81–85
6. Hunter RJ (1989) Foundations of Colloid Science, Vol. I. Clarendon Press, Oxford (a) Appendix A5, (b) Appendix A6
7. Hill TL (1960) An Introduction to Statistical Thermodynamics. Addison-Wesley Publishing Company, Inc, Reading, Chap. 15
8. Alder BJ, Hoover WG, Young DA (1968) J Chem Phys 49:3688–3696
9. Carnahan NF, Starling KE (1969) J Chem Phys 51:635–636
10. Agterof WGM, van Zomeren JAJ, Vrij A (1976) Chem Phys Lett 43:363–367
11. Lyklema J (1991) Fundamentals of Interface and Colloid Science, Vol. I: Fundamentals. Academic Press, London, Chap. 6
12. Hansen J-P, McDonald IR (1976) Theory of simple liquids. Academic Press, London, Chap. 4
13. Vrij A (1980) J Chem Phys 72:3735–3739
14. Buyevich YA, Ivanov AO (1992) Physica A 190:276–294
15. Biben T, Hansen J-P, Barrat J-L (1993) J Chem Phys 98:7330–7344

Received December 15, 1993;
accepted March 17, 1994

Authors' address :

Dr. Michel Martin
Ecole Supérieure de Physique et Chimie Industrielles
Laboratoire de Physique et Mécanique
des Milieux Hétérogènes
(URA CNRS 857)
10, rue Vauquelin
75231 Parix Cedex 05, France